Dental Biometrics: Alignment and Matching of Dental Radiographs

Hong Chen, *Student Member*, *IEEE*, and
Anil K. Jain, *Fellow*, *IEEE*

Abstract—Dental biometrics utilizes dental radiographs for human identification. The dental radiographs provide information about teeth, including tooth contours, relative positions of neighboring teeth, and shapes of the dental work (e.g., crowns, fillings, and bridges). The proposed system has two main stages: feature extraction and matching. The feature extraction stage uses anisotropic diffusion to enhance the images and a Mixture of Gaussians model to segment the dental work. The matching stage has three sequential steps: tooth-level matching, computation of image distances, and subject identification. In the tooth-level matching step, tooth contours are matched using a shape registration method, and the dental work is matched on overlapping areas. The distance between the tooth contours and the distance between the dental work are then combined using posterior probabilities. In the second step, the tooth correspondences between the given query (postmortem) radiograph and the database (antemortem) radiograph are established. A distance based on the corresponding teeth is then used to measure the similarity between the two radiographs. Finally, all the distances between the given postmortem radiographs and the antemortem radiographs that provide candidate identities are combined to establish the identity of the subject associated with the postmortem radiographs.

Index Terms—Dental radiographs, curve alignment, shape registration, spline, biometrics.

1 Introduction

DENTAL records have been extensively used in identifying the victims of massive disasters, such as the 9/11 bombing and the Asian tsunami [1], [2]. So, the importance of using dental records for human identification is now well recognized. Dental Biometrics uses dental radiographs to identify victims in situations (e.g., fire victims) where conventional biometric features, i.e., face, fingerprint, and iris, are not available [3]. The radiographs acquired after the victim's death are called postmortem (PM) radiographs, and the radiographs acquired while the victim is alive are called antemortem (AM) radiographs (Fig. 1). Generally, information from the victim's body or the scene provides some clues about the tentative identity of the victim. Based on this information, specific AM radiographs, labeled with patient names, can be obtained from the dentists. The goal of dental biometrics is to match an unidentified individual's PM radiographs against a database of labeled AM radiographs. If the teeth in the PM radiographs sufficiently match the teeth in someone's AM radiographs, the identity of the PM radiographs is established.

Previous work reported in the literature [4], [5] only used the contours of teeth for identification. The matching algorithm in this paper utilizes both the contours of teeth and the shapes of the dental work (e.g., fillings, crowns, and bridges). Furthermore, this paper presents a systematic approach for establishing a similarity measure between the unidentified PM subject and the AM subjects in the database. As Fig. 2 shows, the procedure of matching a query PM subject to a database AM subject is as follows: At the tooth-level matching stage, every pair of neighboring teeth in PM images are matched to all pairs of neighboring teeth in AM images, based on tooth contours and dental work, and the matching scores are fused; on the basis of the fused matching scores, the tooth correspondence is established for each pair of PM-AM images, and a distance representing the dissimilarity between the PM image and the AM image is computed; the third stage utilizes the distances between images to infer the identity associated with the PM images. A system diagram is shown in Fig. 3.

• *The authors are with the Department of Computer Science and Engineering, Michigan State University, 3115 Engineering Building, East Lansing, MI 48824. E-mail: {chenhon2, jain}@cse.msu.edu.*

Manuscript received 7 July 2004; revised 4 Feb. 2005; accepted 8 Feb. 2005; published online 13 June 2005.
Recommended for acceptance by M. Pietikainen.
For information on obtaining reprints of this article, please send e-mail to: tpami@computer.org, and reference IEEECS Log Number TPAMI-0338-0704.

2 Feature Extraction

The methods for extraction of tooth contours along with some preprocessing procedures, i.e., radiograph segmentation and gumline detection, have been presented in the literature [4], [5], [6]. We use the active contour model for extraction of the tooth contours [5]. Fig. 4 shows some examples of the extracted tooth contours.

The dental work, which appears as bright regions in the radiographs, is another salient feature for subject identification (Fig. 1). To extract the contours of the dental work, the intensity histogram of the tooth image is approximated with a Mixture of Gaussians model [7]—the Gaussian component with the largest mean value corresponds to the pixels associated with the dental work (see Fig. 5). The dental work is segmented by thresholding the image using a threshold which separates the dental work component from the other components for the smallest classification error [8], [9].

Intuitively, as the variances of the Gaussians decrease, the classification error (dental work pixels versus tooth pixels) decreases as well because there will be less overlap between the Gaussians. From the viewpoint of image processing, reduction of the variance of each component is equivalent to smoothing the pixels inside each region while preserving the boundary between the regions. The anisotropic diffusion [10], [11], [12], [13] is used for this purpose. Fig. 6 shows some images and the segmented dental work before and after the anisotropic diffusion.

3 Matching at Tooth Level

A pair of neighboring teeth are viewed as a unit in matching. The contours of teeth are matched using a shape registration method, and the dental work is matched in the overlapping areas of the teeth. These two matching scores are then combined using posterior probabilities.

3.1 Matching Tooth Contours

A contour matching algorithm was presented in the previous work [4]. This algorithm aligns the contours and calculates the average distance between all points in the query shape and their closest points in the database shape and uses it to represent the distance between tooth contours. However, if one of the contours has some missing points due to occlusion or poor image quality, the algorithm fails to align the partial contour to the complete contour. The algorithm proposed in this paper solves this problem by establishing the point correspondence between the two curves and

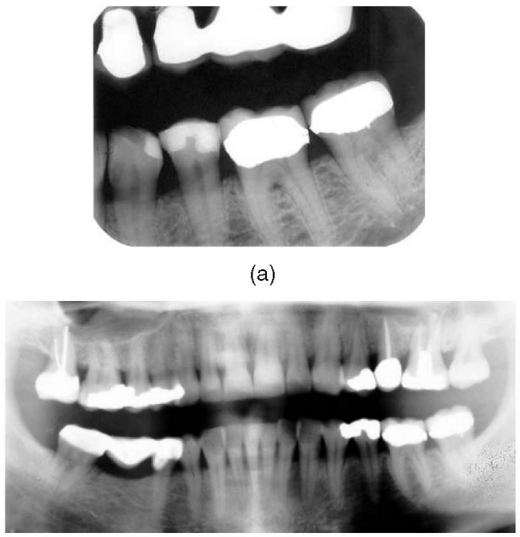

Fig. 1. Matching postmortem (PM) images to the database of antemortem (AM) images. The identity of the PM radiograph in (a) is the same as the identity of the AM radiograph in (b). The dental work, e.g., crowns, fillings, and bridges, is shown as bright regions.

then computing the distances between the curves on the basis of the corresponding points.

Denote the given tooth contours as A and B. A contains the contours of a pair of neighboring teeth in a PM image, and B contains the contours of a pair of neighboring teeth in an AM image (see Fig. 7a). The neighboring teeth are viewed as a unit in matching, which has the advantage that not only the contours but also their relative positions contribute to the matching. The first step is to sample continuous shapes A and B into point sets AP and BP. In order to find the correspondence from AP to BP, the sampling rate for B should be sufficiently high so that BP can approximate B precisely enough for distance computation (see Fig. 7b). We use the Arc Length Parametrization method to generate equidistanced points [14].

A transformation is used to align the contours. Let the rotation angle be θ, the translations along the x and y axes be t_x and t_y, respectively, and the scaling be s. A point $(x, y)^t$ is transformed to $T(x, y)$, where

$$T(x,y) = s\begin{pmatrix}\cos\theta & -\sin\theta \\ \sin\theta & \cos\theta\end{pmatrix}\begin{pmatrix}x \\ y\end{pmatrix} + \begin{pmatrix}t_x \\ t_y\end{pmatrix}. \quad (1)$$

The optimal transformation T minimizes the matching distance, which is computed after shape registration. To initialize T, both A and B are normalized so that their bounding boxes have the same widths (Fig. 7c).

Denote the transformation from AP to BP as T. The *Shape registration* stage establishes the correspondence from $T(AP)$ to BP, which preserves the topologies on the two curves, i.e., if $i < j$ and a_i and a_j correspond to b_k and b_l, respectively, then $k < l$, where a_i, $a_j \in T(AP)$ and b_k, $b_l \in BP$ [15]. Because the two curves may not fully overlap, the *outliers*, which do not have corresponding points in the counterpart curve, are present. The shape registration algorithm, which detects the outliers, is given as follows:

Algorithm: Shape Registration

Input: two ordered point sets TAP and BP, where TAP is the transformed version of AP, i.e., $TAP = T(AP)$. The kth point in TAP is denoted as $TAP(k)$ and the kth point in BP is denoted as $BP(k)$.

Goal: to find the correspondence from TAP to BP, which is denoted as $Cor(i)$, where $i = 1, ..., |TAP|$, and $1 \le Cor(i) \le |BP|$. The notation $|\cdot|$ denotes the number of elements in the set.

1. Initialization: Initialize $Cor(\cdot)$ as $Cor(i) = \lfloor \frac{|BP|}{|TAP|}(i-1)+1 \rfloor$, where $i = 1, ..., |TAP|$, and $\lfloor m \rfloor$ means the greatest integer below m. For convenience of description, we add two elements to $Cor(\cdot)$, i.e., $Cor(0) = 1$ and $Cor(|TAP|+1) = |B|$.

2. For $i = 1..|TAP|$ do

$$Cor(i) \leftarrow \arg \min_{k=Cor(i-1)}^{Cor(i+1)} \|TAP(i) - BP(k)\|;$$
$$Dis(i) \leftarrow \|TAP(i) - Cor(i)\|.$$

3. Repeat step 2 until a convergence or a maximum number of iterations is reached.

4. If some adjacent points in TAP correspond to the same point in BP, i.e., $Cor(i) = Cor(i+1) = ... = Cor(i+k)$, and $p = \arg\min_{k=i..i+k} Dis(k)$, then $Cor(i) = nil, \forall i \ne p$. The points for which $Cor(i) = nil$ are the outliers (Fig. 7(f)).

Denote the points in TAP that have corresponding points as TAP'. The distance between tooth contours A and B is given as $d_t(A, B)$, where

$$d_t(A,B) = \min_{\forall T} \frac{1}{|TAP'|} \sum_{\text{all } a' \in TAP'} \|T(a') - Cor(a')\|. \quad (2)$$

$d_t(A, B)$ is minimized by searching for the optimal parameters of T. This optimization problem is solved iteratively using Sequential Quadratic Programming [16]. Since $Cor(\cdot)$ is affected by T, the correspondence is established at each optimizing iteration.

3.2 Matching Dental Work

The dental work is another feature for matching dental radiographs. Due to the difficulty in matching the contours of the dental work (Figs. 8a, 8b, and 8c), a metric based on the regions of the dental work is used.

The preprocessing stage sets the pixels inside the tooth contours to be 0 and then the pixels inside the contours of the dental work to be 1 (See Figs. 8d and 8e). Given two images M and N, the relative number of misaligned pixels (n_{mp}) is defined as:

$$n_{mp}(M,N) = \frac{\sum_{i,j} M'(i,j) \bigoplus N'(i,j)}{\sum_{i,j} M'(i,j) + N'(i,j)}, \quad (3)$$

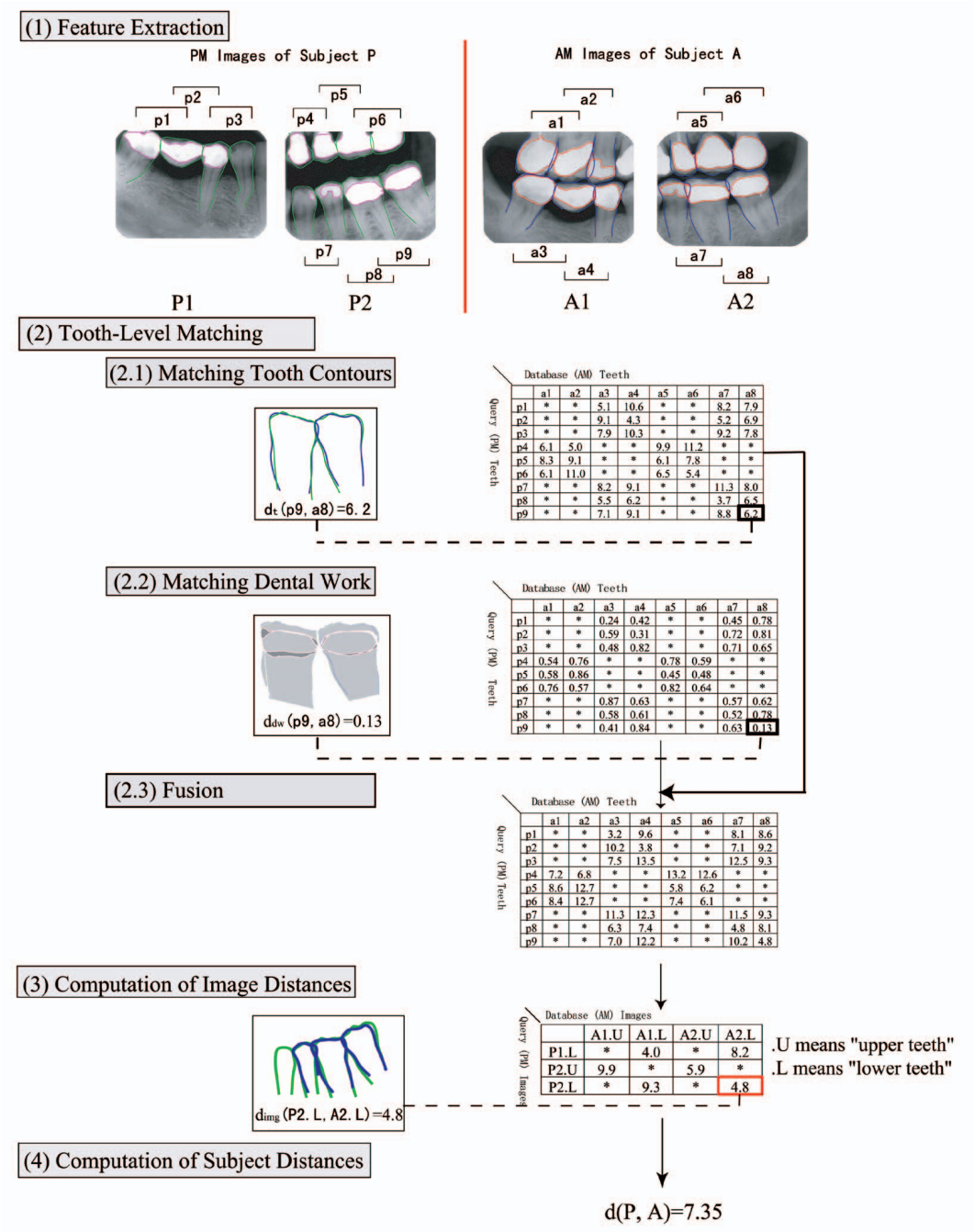

Fig. 2. Process of matching subject P's PM radiographs, P1 and P2, with subject A's AM radiographs, A1 and A2. Note that p1, ..., p8 are neighboring teeth in PM images, and a1, ..., a8 are neighboring teeth in AM images. (*) in the tables stands for a matching between lower PM teeth and upper AM teeth, or a matching between upper PM teeth and lower AM teeth.

where M' and N' are results of the preprocessing on M and N, and $\oplus$ is the "exclusive-or" operator. The metric n_{mp} is used to measure the alignment of the dental work. If the dental works in images M and N have similar shapes and are well aligned, then n_{mp} is small. So, the distance between the dental work in images M and N is defined as

$$d_{dw}(M, N) = \min_{\forall T} n_{mp}(T(M), N), \tag{4}$$

where T is based on the transformation defined in (1) and (2). In other words, the optimum parameters of T for matching tooth contours in (1) and (2) are the initialization values for (4).

3.3 Fusion of d_t and d_{dw}

The distance d_t, which measures the difference between contours of teeth, and distance d_{dw}, which measures the difference between regions of the dental work, are combined to obtain a better similarity measure. However, d_{dw} is not available for the teeth that do not have dental work. This problem is solved by using posterior probabilities.

Let ω_g represent the matching between radiographs of the same subject (genuine class) and ω_i represent the matching between radiographs belonging to two different subjects (imposter class). The likelihood distributions of d_{dw} for genuine and imposter classes, $p(d_{dw}|\omega_g)$ and $p(d_{dw}|\omega_i)$, were computed over nearly

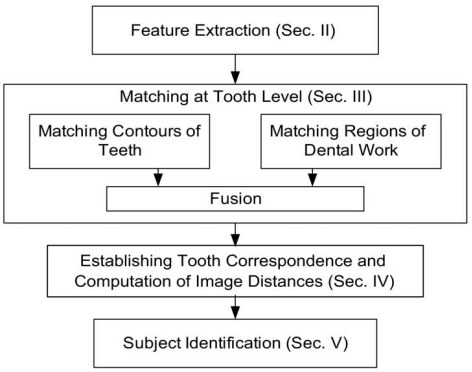

Fig. 3. Diagram of the proposed system.

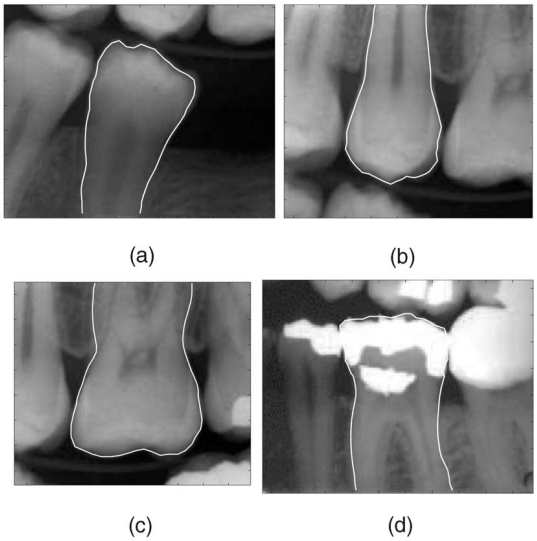

Fig. 4. Some examples of extracted tooth shapes.

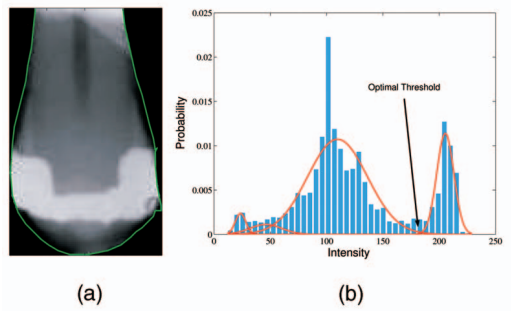

Fig. 5. Fitting a Mixture of Gaussians model (with four components) to the intensity histogram (b) of an image (a). The rightmost peak in (b) corresponds to the dental work. The other peaks correspond to intensity variations inside the tooth.

100 representative images (shown in Fig. 9). A Parzen window approach with a Gaussian kernel was used to estimate the probability distributions, $p(d_{dw}|\omega_i)$ and $p(d_{dw}|\omega_g)$. The two posterior probabilities are

$$P(\omega_i|d_{dw}) = \frac{p(d_{dw}|\omega_i)P(\omega_i)}{p(d_{dw})}, \quad (5)$$

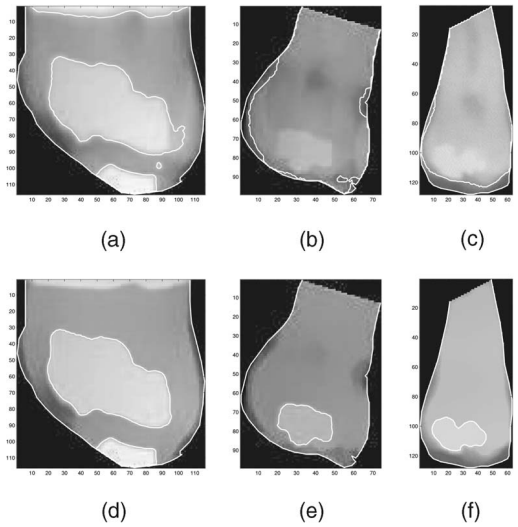

Fig. 6. The original images and the extracted contours of dental work ((a), (b), (c)). The corresponding smoothed images and the extracted contours are shown in (d), (e), and (f).

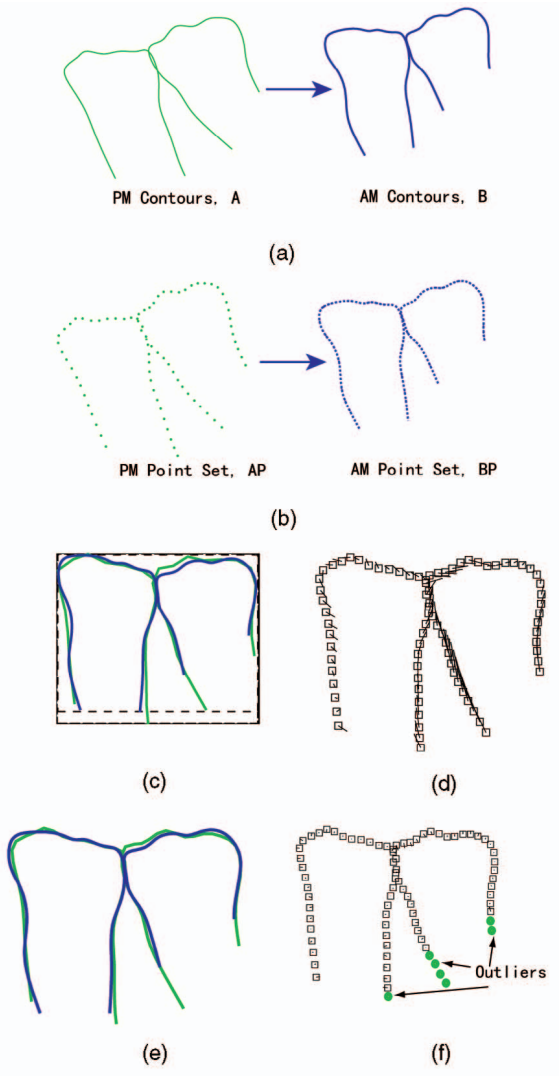

Fig. 7. Process of shape registration. (a) Continuous tooth contours. (b) Discrete tooth contours. (c) Initialization by aligning bounding boxes. (d) The initialized point correspondence. (e) Aligned contours after optimum transformation. (f) Correspondence after alignment and detected outliers.

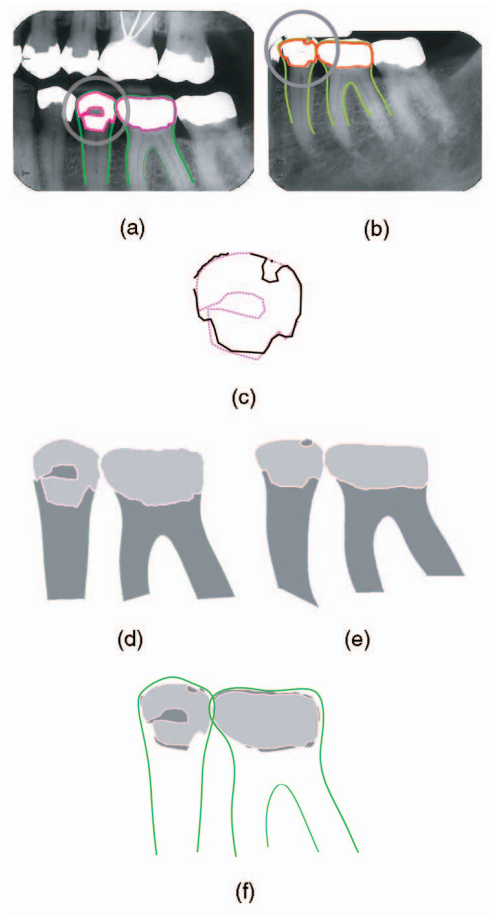

Fig. 8. Dental work merging due to a change in the imaging angle. The hole in the circled dental work seen in image (a) is occluded when viewed from the angle shown in (b) even though both the images are of the same tooth. (c) The contours of the dental work shown in (a) and (b) are aligned. (d) The preprocessed image for the tooth in image (a). (e) The preprocessed image for the tooth in image (b). (f) The alignment of the dental work.

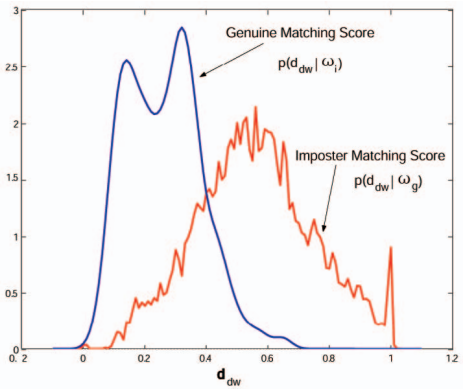

Fig. 9. The distributions of matching distances based on shapes of the dental work.

$$P(\omega_g|d_{dw}) = \frac{p(d_{dw}|\omega_g)P(\omega_g)}{p(d_{dw})}, \tag{6}$$

where the priors, $P(\omega_i)$ and $P(\omega_g)$, are assumed to be 0.5. The prior probability $p(d_{dw})$ is defined as $p(d_{dw}) = 0.5 \cdot [p(d_{dw}|\omega_i) + p(d_{dw}|\omega_g)]$.

The matching distance d_t (between teeth contours) is combined with distance d_{dw} (between dental work) to generate the distance d_f between the two teeth-pairs A and B, which is given by

$$d_f(A,B) = d_t(A,B) \cdot (1 + (T(d_{dw}))), \tag{7}$$

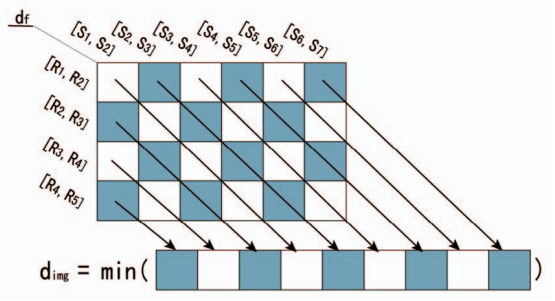

Fig. 10. Coupling four pairs of neighboring teeth with six pairs of neighboring teeth. The matching score between each pair of neighboring teeth is calculated and the average is taken along the arrows. The results are listed in the lower black and white cells, and the minimum of these values is defined as the matching distance between the two images.

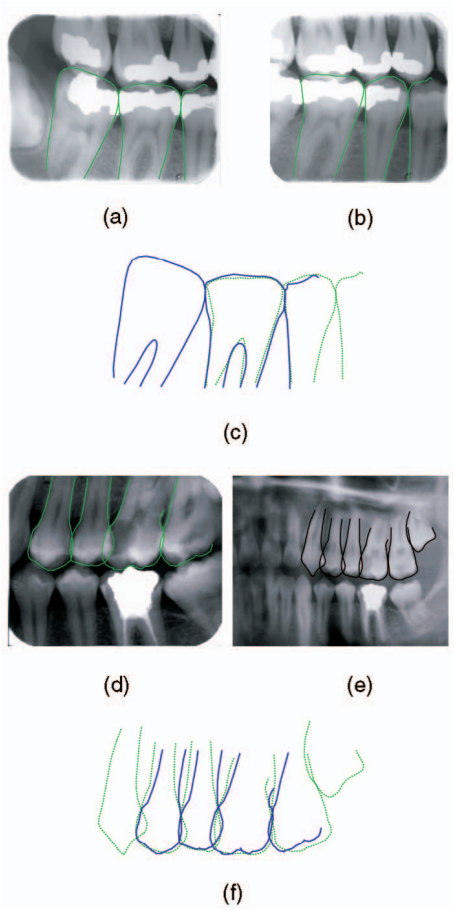

Fig. 11. Two examples of tooth correspondence. The tooth contours in (a) and (b) are paired up in (c). The tooth contours in (d) and (e) are paired up in (f).

$$T(d_{dw}) = \begin{cases} P(\omega_i|d_{dw}) - P(\omega_g|d_{dw}), & \text{if } d_{dw} \text{ is available;} \\ 0, & \text{otherwise.} \end{cases} \tag{8}$$

The above combination scheme implies that, if d_{dw} is more likely to be the distance between the genuine teeth, d_t is reduced; if d_{dw} is more likely to be the distance between imposter teeth, d_t is amplified; if d_{dw} is not available, d_t is not changed.

4 Tooth Correspondence and Distance between Images

We view teeth in different rows as different images. The matching distance between images should rely on the corresponding teeth

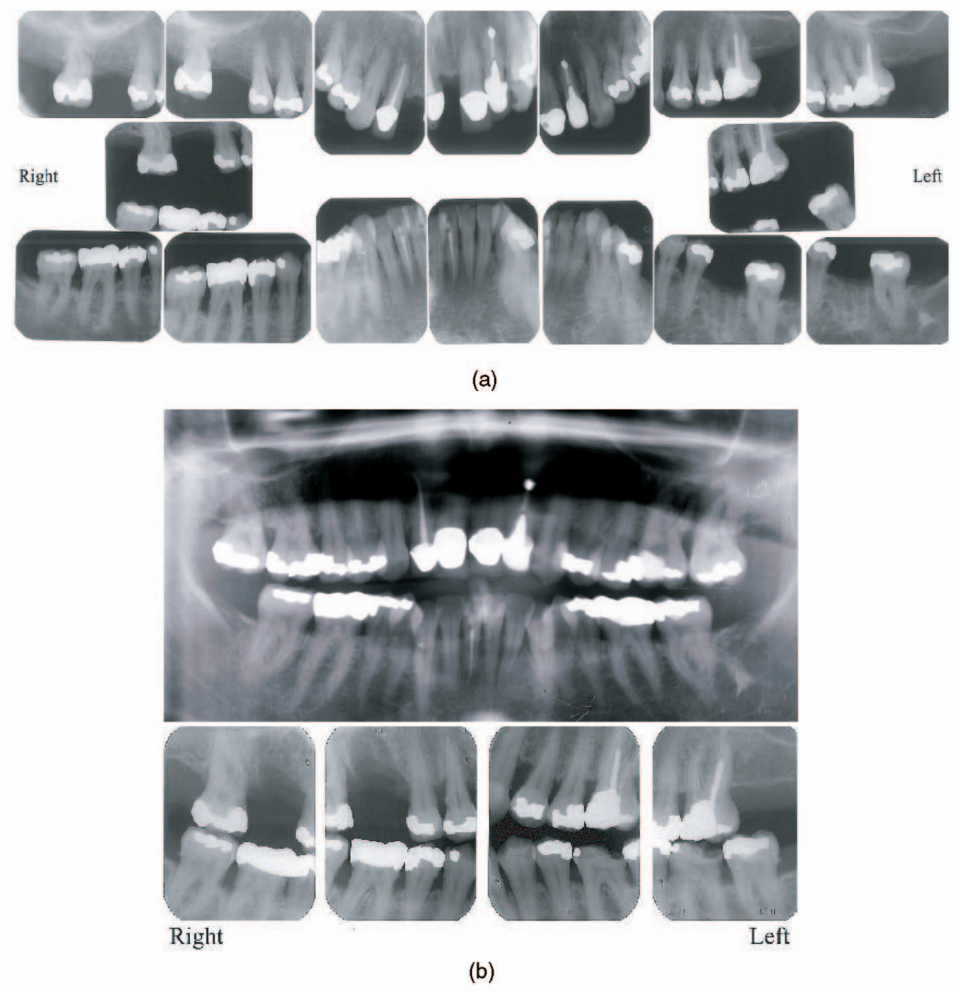

Fig. 12. For a subject in the database, there are PM images acquired on 08/06/2003 (a) and AM images acquired on 10/13/99 (b).

only. Establishing tooth correspondence between images is the main task at this stage. We assume that no teeth are missing between the acquisitions of AM and PM images; so, for neighboring teeth in AM images, their corresponding teeth in PM images should be neighbors as well.

The following algorithm uses the results of the tooth-level matching to establish the correspondence between two images R and S. The numbers of teeth in R and S are not necessarily the same. Suppose a possible tooth correspondence starts from the ith tooth in R and the jth tooth in S ($i = 1$ or $j = 1$), so it is denoted as $\mathbb{C} = \{(R_i, S_j), (R_{i+1}, S_{j+1}), \ldots, (R_{i+l}, S_{j+l})\}$, where R_{i+k} is the corresponding tooth of S_{j+k}, $k = 0, \ldots, l$. Then, the correct tooth correspondence should minimize the average distance between the corresponding teeth, which is defined as:

$$d_{img}(R, S) = \min_{\substack{\forall i,j, \\ i=1 \\ \text{or } j=1}} \frac{1}{l} \sum_{k=0}^{l-1} d_f([R_{i+k}, R_{i+k+1}], [S_{i+k}, S_{i+k+1}]), \quad (9)$$

where $[.,.]$ means that the contours of neighboring teeth are concatenated and matched as a unit, as discussed in Section 3. Fig. 10 illustrates the computation of d_{img} in matching a 5-tooth image to a 7-tooth image. Fig. 11 shows some correctly established tooth correspondences.

5 Subject Identification

Given the matching distances between two images, the similarities between subjects are computed. Suppose U is a subject to be identified and denote the PM images for U as $u_1, u_2, \ldots, u_m$. Label the ith subject in the AM database as V^i, $i = 1, \ldots, k$. Denote the AM images for subject V^i as $v_1^i, v_2^i, \ldots, v_{n_i}^i$. The algorithm for subject identification has two steps. The first step is to compute the matching distances between one PM image u_p and all the AM images of V^i. If two images do not have any tooth in common, their matching distance will be large. Only if the images have some teeth in common and the correspondence is correct will the matching distance be small. So, the smallest matching distance is chosen to represent the matching distance between the image u_p and the subject V^i, i.e.,

$$d_{img\_sub}(u_p, V^i) = \min_{q=1..n_i} d_{img}(u_p, v_q^i). \quad (10)$$

In the second step, the image-to-subject distances are averaged over all images of subject U to obtain the matching distance between U and V^i, that is

$$d(U, V^i) = \frac{1}{m} \sum_{p=1..m} d_{img\_sub}(u_p, V^i). \quad (11)$$

Given the distances between the unidentified subject and all the subjects in the AM database, a candidates list is generated by ranking these distances.

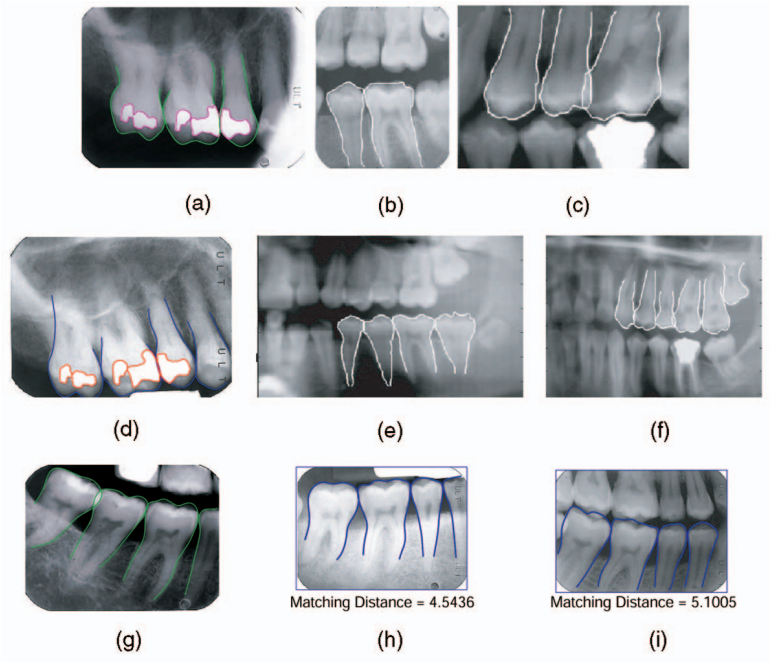

Fig. 13. Some pairs of successful retrievals ((a) and (d), (b) and (e), (c) and (f)) and an unsuccessful retrieval ((g), (h), (i)). Due to the resemblance of the shapes, (g) is incorrectly matched to (h) which belongs to another subject. The genuine match for (g), shown in (i), is ranked as the second closest match.

6 Experimental Results

To evaluate our algorithms, we need a database containing both AM and PM images. PM dental radiographs are much more difficult to obtain than AM radiographs. We have access to a small database from the FBI's Criminal Justice Information Service (CJIS) division, which is interested in utilizing dental radiographs for identifying Missing and Unidentified Persons (MUPs). Fig. 12 shows some of the AM and PM images in the database.

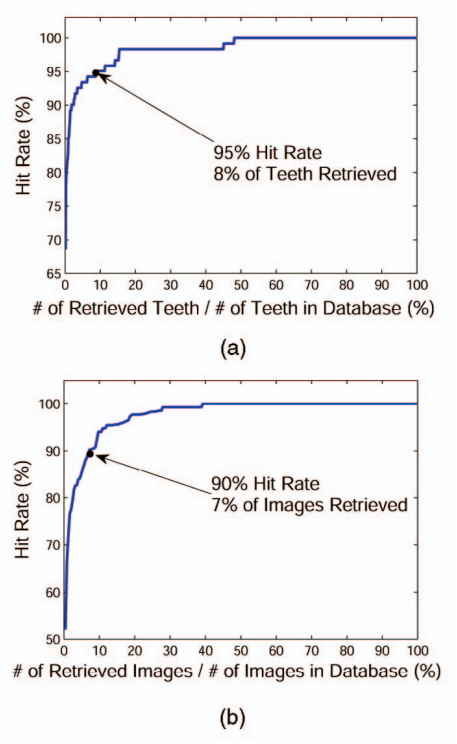

Fig. 14. (a) Retrieval of PM teeth from the database of AM teeth after shape registration. (b) Accuracy of retrieval of PM images from the database of AM images (b).

There are 25 subjects in our database, each having a number of AM and PM images. Because 14 of the 25 subjects in the database have the problems of 1) unreliable tooth contours due to poor image quality, 2) variation of dental structure due to tooth development or orthodontic treatment, or 3) insufficient number of AM images for matching, we did not try to establish the identities of these 14 subjects. Instead, the AM images of these 14 subjects served as the hoax identities in the database. So, we matched the 11 subjects (166 PM images) to all 25 subjects (235 AM images) in the database.

The dental radiographs were matched in three steps. The first step of matching is at the tooth level. There are 414 PM teeth and 738 AM teeth in the matching. The result of matching against the whole database showed that, in 95 percent of the cases, genuine teeth were among the top 8 percent of the retrieved images (see Fig. 14a).

In the second step, teeth in the same rows are viewed as a unit. One hundred sixty-six PM images are matched against 235 AM images. If PM teeth are matched with the same person's AM image and the tooth correspondence is correct, we call it a successful match. Some examples of successful and unsuccessful matchings are shown in Fig. 13. The ROC curve in Fig. 14b shows that, in 90 percent of the cases, the genuine images were among the top 7 percent of the retrievals.

The purpose of matching dental radiographs was to obtain an individual's identity, so the final stage was to identify the subjects. In this step, 11 PM subjects were matched to the 25 AM subjects. As Fig. 15 shows, the accuracy curve of retrieving 11 subjects from the database of 25 subjects is shown in the figure. Using the top-1 retrieval, the accuracy is 8/11 (= 72 percent). Using top-4 retrievals, which recalls 16 percent of all the subjects, the retrieving accuracy is 91 percent. The accuracy reaches 100 percent when the top-7 retrievals are used.

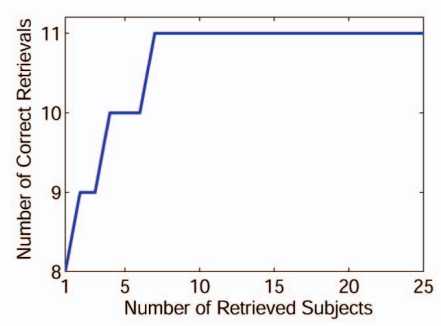

Fig. 15. Identifying 11 PM subjects, each with 25 possible identities.

7 Conclusions

Dental biometrics is used to identify individuals in the forensic domain. This paper presents an automatic method for matching dental radiographs. The matching is performed in three steps. In the first step, a shape registration method aligns the tooth contours and computes the distance between them. If dental work is present, an area-based metric is used for matching the dental work. The two matching distances are then combined using posterior probabilities. In the second step, the tooth correspondence is established for a PM and an AM image and it is used to compute the similarity between the pair of images. In the third step, the distances between subjects are computed and used to retrieve the identities from the database. Experimental results show that this approach is promising.

There are still a number of challenges to overcome. The shape extraction is a difficult problem for dental radiographs, especially for poor quality images where some tooth contours are indiscernible. For subjects with missing teeth, we are exploring other features for identification, such as the shape of mandibular canals and maxillary sinus. We are also in the process of obtaining a larger database for evaluating the algorithm.

Acknowledgments

This research was supported by US National Science Foundation grant EIA-0131079.

References

[1] P. O'Shaughnessy, "More than Half of Victims IDD," *New York Daily News,* Sept. 2002.
[2] P. Thepgumpanat, "Thai Tsunami Forensic Centre Produces First IDs," *Reuters,* http://www.alertnet.org/, Jan. 2005.
[3] I.A. Pretty and D. Sweet, "A Look at Forensic Dentistry—Part 1: The Role of Teeth in the Determination of Human Identity," *British Dental J.,* vol. 190, no. 7, pp. 359-366, Apr. 2001.
[4] A.K. Jain and H. Chen, "Matching of Dental X-Ray Images for Human Identification," *Pattern Recognition,* vol. 37, no. 7, pp. 1519-1532, 2004.
[5] H. Chen and A.K. Jain, "Tooth Contour Extraction for Matching Dental Radiographs," *Proc. 17th Int'l Conf. Pattern Recognition,* vol. III, pp. 522-525, Aug. 2004.
[6] J. Zhou and M. Abdel-Mottaleb, "Automatic Human Identification Based on Dental X-Ray Images," *Proc. SPIE Technologies for Homeland Security and Law Enforcement Conf.,* Apr. 2004.
[7] M. Figueiredo and A.K. Jain, "Unsupervised Learning of Finite Mixture Models," *IEEE Trans. Pattern Analysis and Machine Intelligence,* vol. 24, no. 3, pp. 381-396, Mar. 2002.
[8] R.C. Gonzalez and P. Wintz, *Digital Image Processing.* Addison-Wesley, 1977.
[9] M. Sonka, V. Hlavac, and R. Boyle, *Image Processing—Analysis, and Machine Vision,* second ed. Florence, Ky.: Brooks/Cole, Thomson Learning, 1999.
[10] P. Perona and J. Malik, "Scale-Space and Edge Detection Using Anisotropic Diffusion," *IEEE Trans. Pattern Analysis and Machine Intelligence,* vol. 12, no. 7, pp. 629-639, July 1990.
[11] H. Huang and J. Wang, "Anisotropic Diffusion for Object Segmentation," *Proc. IEEE Int'l Conf. Systems, Man, and Cybernetics,* vol. 3, pp. 1563-1567, Oct. 2000.
[12] Y. Yu and S. Acton, "Speckle Reducing Anisotropic Diffusion," *IEEE Trans. Image Processing,* vol. 11, no. 11, pp. 1260-1270, 2002.
[13] M. Black, G. Sapiro, D. Marimont, and D. Heeger, "Robust Anisotropic Diffusion," *IEEE Trans. Image Processing,* vol. 7, no. 3, pp. 421-432, 1998.
[14] H. Wang, J. Kearney, and K. Atkinson, "Arc-Length Parameterized Spline Curves for Real-Time Simulation," *Proc. Fifth Int'l Conf. Curves and Surfaces,* pp. 387-396, June 2002.
[15] N. Duta, A.K. Jain, and M.-P. Dubuisson-Jolly, "Automatic Construction of 2D Shape Models," *IEEE Trans. Pattern Analysis and Machine Intelligence,* vol. 23, no. 5, pp. 433-446, May 2001.
[16] S. Han, "A Globally Convergent Method for Nonlinear Programming," *J. Optimization Theory and Applications,* vol. 22, p. 297, 1977.